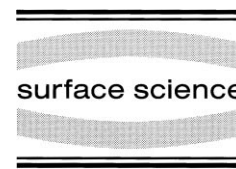




ELSEVIER

Surface Science 464 (2000) 217–222



www.elsevier.nl/locate/susc

Novel dark-field imaging of GaN {0001} surfaces with low-energy electron microscopy

J.B. Maxson, N. Perkins, D.E. Savage, A.R. Woll, L. Zhang, T.F. Kuech,
M.G. Lagally *

University of Wisconsin — Madison, Department of Materials Science & Engineering, 1509 Madison Avenue, Madison, WI 53706, USA

Received 11 February 2000; accepted for publication 19 June 2000

Abstract

We have observed significant dark-field diffraction contrast from adjacent terraces of the GaN (0001) surface in low-energy electron microscopy, an unexpected result, as the surface is not reconstructed and thus has no superlattice reflections. Calculations show that the contrast originates from a 60° rotation of the hexagonal unit cell across odd-multiple bilayer-high steps. The result is general: the terrace morphology from any {0001} surface of wurtzite structures can be simply imaged even if the surface is not reconstructed. © 2000 Elsevier Science B.V. All rights reserved.

Keywords: Electron–solid diffraction; Gallium nitride; Low energy electron diffraction (LEED); Low-energy electron microscopy (LEEM); Low index single crystal surfaces; Semiconducting films; Surface structure, morphology, roughness, and topography

The surface morphology of a deposited film can play a key role in the operation of electronic devices, especially those that are based on ultra-thin layers [e.g. multi-quantum well (MQW) light emitting diodes and lasers]. The resulting interfacial roughness when a layer is buried can significantly influence electronic and optoelectronic behavior. This effect is well-known [1] and has recently been observed $\text{In}_x\text{Ga}_{1-x}\text{N}/\text{GaN}$ MQWs [2]. Currently, there is a strong push for high-quality large-bandgap devices made from group III-nitrides [3–5]. An understanding of the progression of surface morphology during growth of these materials will help to produce higher-quality interfaces.

Low-energy electron microscopy (LEEM) is a

powerful technique for studying surface morphology and its evolution. LEEM can provide in-situ, real-time surface characterization during growth at high temperature both in real space and in reciprocal space. When used as an imaging technique, local surface changes (e.g. island shape [6] or dislocation strain fields [7]) can be observed during growth. Used as a diffraction tool, variations of the overall surface atomic arrangement within the field of view can be determined. LEEM is thus well suited to provide important surface morphological data from the initial adatom deposition and nucleation of islands throughout the film's growth.

In LEEM, as with all electron microscopies, understanding the basis of contrast is imperative to the correct interpretation of acquired images. Two major classifications of contrast in LEEM are interference contrast and diffraction contrast.

* Corresponding author. Fax: +1-608-265-4118.

E-mail address: lagally@neep.engr.wisc.edu (M.G. Lagally)

Interference contrast results from the change of phase of the incident and reflected electron waves (e.g. at an atomic step or from the top and bottom surfaces of an extremely thin film) [8]. Commonly performed in bright field (using the specularly reflected beam for imaging), this technique emphasizes the abrupt change in surface height occurring at a step, representing it as a line on a uniform background. The step's image characteristics while varying focus and energy can provide the height of a step and the sense of the step (direction of 'up-step') as well [8–13]. Diffraction contrast, as the name implies, is generated by using a diffracted beam for imaging (i.e. dark-field), providing contrast between surface regions that have different structure and thus contribute to this beam in different ways. Diffraction contrast, for example, shows areas of different reconstruction with high contrast. A well-known example is $p(2 \times 1)/p(1 \times 2)$ Si(001). If a half-order superstructure beam is used for imaging, adjacent terraces separated by a monolayer-high step are represented in the LEEM image with inverted contrast (black to white) because of the 90° rotation of the surface reconstruction upon crossing this step [14]. Once the origin of contrast is understood, diffraction contrast can provide immediate feedback on the location of steps and their height as a function of atomic-layer thickness, as well as changes of the reconstruction *within* the terrace. The sense of the step may be identified from its direction of motion during growth or removal of material.

It would be beneficial to use diffraction contrast imaging for GaN studies as well, as it could allow direct acquisition and interpretation of step location and height information, and possibly the determination of inhomogeneities within and between terraces. Traditional diffraction-contrast LEEM imaging requires the use of a superstructure beam; however, under common MBE growth conditions, the GaN(0001) growth front is simply a (1×1) unreconstructed surface [15]. Because no superstructure exists, this traditional dark-field technique is impossible for diffraction-contrast imaging. Yet, one can image the GaN{0001} surface using the dark-field contrast method, as we show here. (Previous reports of LEEM studies of the GaN surface have not discussed the details of

the contrast mechanism used. See Refs. [16,17].) In this report, we present an explanation for this result. We show that the bulk properties of the material, rather than a surface reconstruction, allow this contrast, extending the capabilities of LEEM to provide single-bilayer vertical resolution in GaN{0001}. The contrast mechanism is general and can be implemented on {0001} surfaces of any würtzite material.

GaN films were deposited in a horizontal-flow metallorganic vapor phase epitaxy reactor from trimethylgallium and ammonia onto epi-polished basal-plane sapphire coated with an AlN buffer layer. Atomic force microscopy (AFM) of these samples shows that the surface consists of flat terraces ~ 250 nm wide, separated by half- and full-unit cell steps that meander across the surface (a unit cell is made of two Ga–N bilayers). Chemical etching following the procedures of Weyher and co-workers [18] has been used to show that our growth process yields a (0001)-type Ga-polar surface. Samples, cleaned with organic solvents, were imaged with LEEM. (For a descrip-

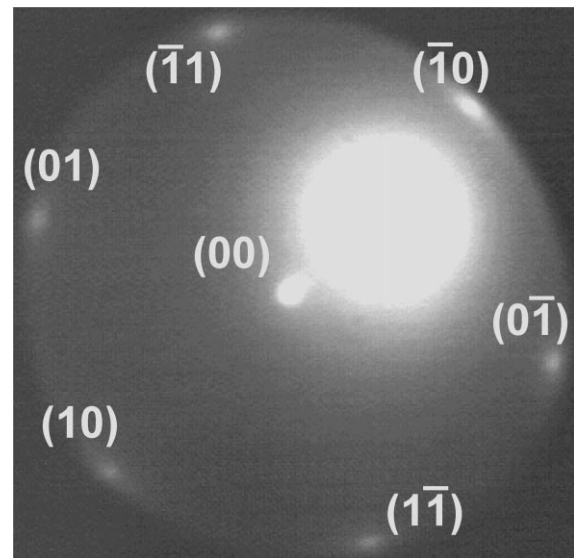


Fig. 1. LEED pattern from GaN(0001) ($E \approx 25$ eV) at room temperature. The first-order diffraction beams show the hexagonal symmetry of the surface. The bright area between the center (00) beam and the $(\bar{1}0)$ beam is due to inelastically scattered electrons. The lack of superlattice reflections shows that the surface is unreconstructed.

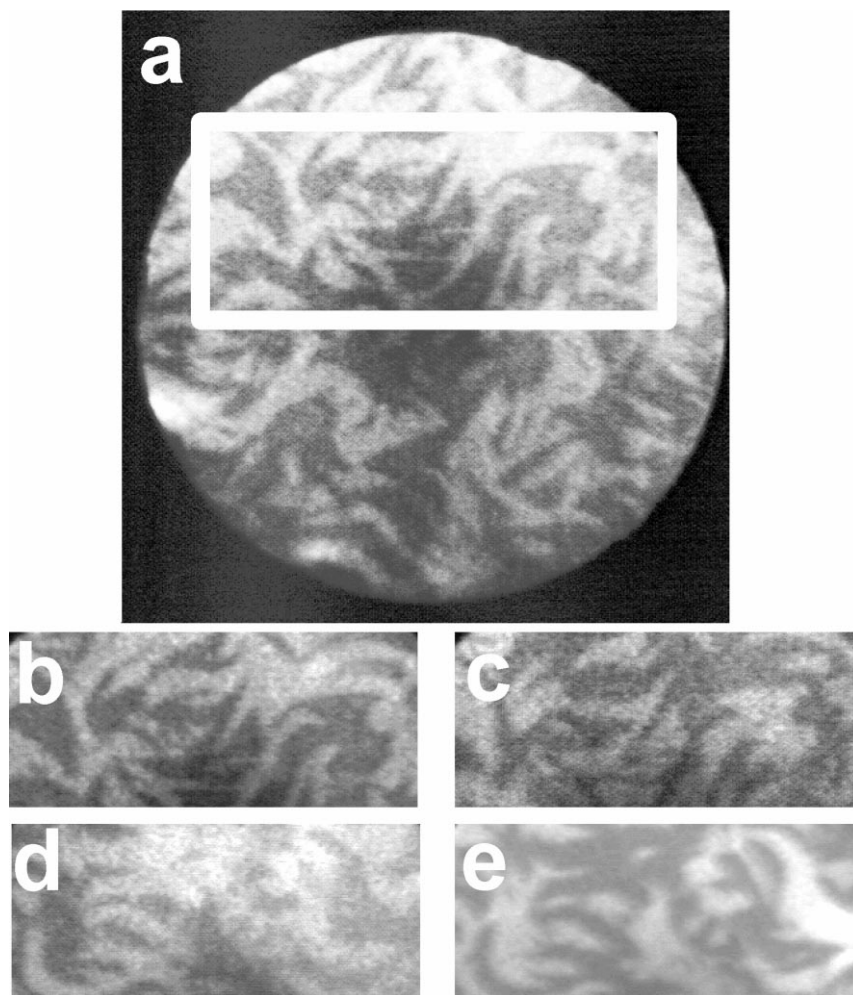


Fig. 2. Dark-field LEEM images taken from GaN(0001) at room temperature. (a) Image taken using the (10) beam. The bright and dark areas represent atomically flat terraces separated by steps with odd-multiple bilayer heights. (b, c) Images taken from the same region of (a) (shown by the $3.5 \times 1.5 \mu\text{m}$ rectangle) but at slightly different energies. (d, e) Dark-field images taken with (10) and $(\bar{1}\bar{1})$ beams, respectively (see Fig. 1 for reference beams), from a different region of the sample. Note the contrast inversion from (b) to (c) and from (d) to (e).

tion of our microscope, see Ref. [19].) LEEM was performed additionally on samples that were annealed in UHV at 400°C for 5 min. Both annealed and unannealed samples show the same characteristics, with the annealed samples yielding slightly higher-contrast images and less background in the diffraction pattern.

The diffraction pattern, shown in Fig. 1, indicates that GaN(0001) is unreconstructed. For dark-field imaging, the incident electron beam

enters the surface at an off-normal angle to bring a desired first-order diffraction beam near the optical axis of the microscope's projection column and through the diffraction aperture.

Example images obtained in this dark-field mode are shown in Fig. 2. Fig. 2a–c shows images using the (10) diffraction beam. (b) is simply a $3.5 \times 1.5 \mu\text{m}$ crop of (a) denoted by the superimposed rectangle, and (c) is taken from the same area as (b) but at a slightly ($\sim 5 \text{ eV}$) higher energy.

The images in Fig. 2d and e, from a different sample location than (a)–(c), are taken at the same beam energy but using the (10) and (11) low-energy electron diffraction (LEED) reflections, respectively; the only difference in the imaging condition between (c) and (d) is that the in-plane component of the incident beam is azimuthally rotated 60°.

As there are no reconstruction domains present to distinguish one region of the sample from another, contrast is not expected on the basis of the standard LEEM dark-field techniques that use superstructure beams for imaging. Careful analysis of the diffraction indicates why this contrast nevertheless occurs and why it inverts both by changing beam energy and changing imaging beam. Consider the near-surface region of the GaN{0001} structure, as seen schematically in Fig. 3. The würtzite unit cell of GaN contains four planes of atoms parallel to the crystallographic basal plane. The tetrahedral bonding arrangement within the cell forces the layers to form two sets of equivalent but rotated and translated bilayers. If we assume a Ga-polar (0001) surface termination, then the GaN(0001) surface structure has three Ga–N bonds between the surface Ga atom and its nearest neighbors in the second layer. However, because of the 60° rotation of the planes with each change of $1/2\text{-}c$ in height, the atom

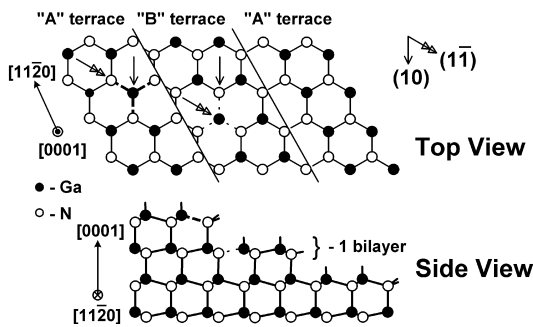


Fig. 3. Schematic drawing of the clean, stepped, unreconstructed GaN(0001) surface. The upper portion of the diagram shows a top view of the surface with the orientation as noted. Barbed arrows show incident-electron k -vectors following the conventions in the text and in Fig. 1. The lower portion of the diagram is a view of the surface layers looking down the [1120] axis. One Ga–N bilayer step height is equal to one-half the GaN c -axis lattice constant ($c=5.185\text{ \AA}$).

locations for the second bilayer are in different positions relative to the adjacent bilayer. This difference allows us to define the terraces arbitrarily as 'A'- and 'B'-type.

The contrast inversion and its occurrence due to a change of imaging beam can be qualitatively explained in terms of simple kinematic diffraction theory. Although the atomic scattering factors can be very different in LEED [20,21], as a very crude approximation, the atomic scattering factor scales with the atomic number. Using the standard formula for the structure factor

$$S_r = \sum_n f_n e^{2\pi i q \cdot r}$$

with f_n equal to the atomic number, q as the reflected wavevector, and r the position of atom n within the unit cell, we show in Fig. 4a) that there

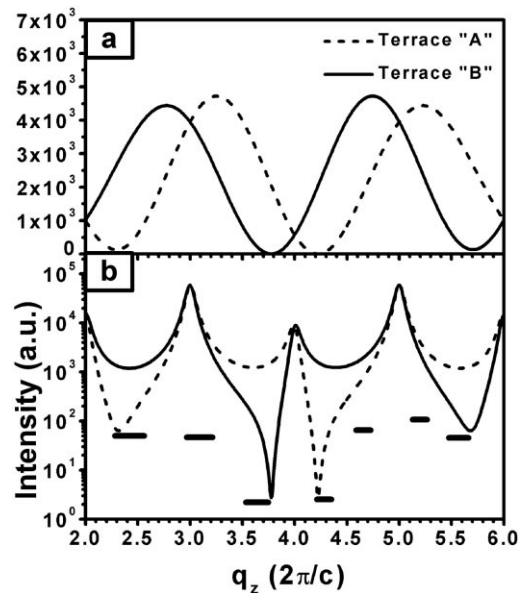


Fig. 4. (a) Squares of the terrace structure factors along a (10) reciprocal-lattice rod for GaN(0001) with A and B-type termination, for a semi-infinite crystal. (b) Kinematic calculation, including an absorption term, of the intensity variation along the (10) rod with energy. At certain energies, the intensities can be remarkably different. A calculation for the (01) beam would show the same behavior with the terraces reversed. The solid horizontal lines represent the positions along the rod at which a local maximum in image contrast is observed. Their length is the uncertainty in determining this energy. See text for discussion.

is a difference between the square of the structure factor of the two surfaces. Furthermore, we can calculate the intensity of the diffracted beam along the surface diffraction rod and qualitatively compare the difference in intensities using this generalization, assuming a semi-infinite crystal and an attenuation factor [22]. If we choose a $(hkl) = (10z)$ beam emerging from a stepped surface, it is evident (Fig. 4b) that the two terraces can have remarkably different intensities. Thus, at certain energies, contrast will exist between the two types of terraces. Changing to an adjacent fundamental beam for imaging causes the geometric situation, and therefore the contrast, to invert as it samples the surface at an azimuthal exit angle 60° from the original. This is shown clearly in Fig. 2d and e.

The inversion of contrast due to a change in energy shown in Fig. 2b and c is qualitatively shown in Fig. 4 as well, as the type of terrace (A or B) that has more intensity at off-Bragg peak positions changes with energy. However, kinematic arguments cannot account for each inversion seen in the data because of the strong multiple scattering of low-energy electrons. We observe several contrast inversions in the energy range that we have explored. The positions of local maximum contrast are shown in Fig. 4b) as bold horizontal lines. Some of these inversions lie in the proper positions for the inversions according to kinematic theory, but extra ones occur. Their positions could be explained only via a full dynamical LEED calculation.

This type of contrast is general for all $\{0001\}$ würtzite crystals, with a higher contrast for materials for which the atomic-scattering factors of atoms A and B are very different. Because the result above is general for any f_1 and f_2 , both polarities of the structure, (0001) and $(000\bar{1})$, will produce contrast, although the final intensities will be different because of different atomic scattering factor values. The symmetry of cubic systems does not allow this contrast method, as the bulk structures do not differ when a step is crossed.

In summary, we have observed considerable contrast in dark-field low-energy electron microscopy imaging of unreconstructed GaN(0001) using fundamental reflections, contrary to expectations based on observations on cubic crystals. The

contrast shows that under appropriate imaging conditions, LEEM can produce a vertical resolution of a single bilayer on $\{0001\}$ surfaces of the würtzite structure. This ability to view terrace morphology based on the bulk properties of the crystal allows direct step-height interpretation, even when there is no surface reconstruction, extending the potential of LEEM for investigating high-temperature growth in these würtzite materials.

Acknowledgements

J.B.M. greatly appreciates discussions with Volkmar Zielasek. J.B.M. also acknowledges the generous support of the NSF through a Graduate Research Fellowship. This research was supported by the Office of Naval Research. Support for purchase of the LEEM was provided by the NSF through its instrumentation program Grant DMR-9413806 and by ONR.

References

- [1] P. Zhou, H.X. Jiang, R. Bannwart, S.A. Solin, G. Bai, *Phys. Rev. B* 40 (1989) 11862.
- [2] K.C. Zeng, M. Smith, J.Y. Lin, H.X. Jiang, *Appl. Phys. Lett.* 73 (1998) 1724.
- [3] S. Nakamura, *MRS Bull.* 23 (1998) 37.
- [4] S. Nakamura, T. Mukai, M. Senoh, *Appl. Phys. Lett.* 64 (1994) 1687.
- [5] J.C. Carrano, T. Li, P.A. Grudowski, C.J. Eiting, R.D. Dupuis, *J. Appl. Phys.* 83 (1998) 6148.
- [6] N.C. Bartelt, R.M. Tromp, E.D. Williams, *Phys. Rev. Lett.* 73 (1994) 1656.
- [7] P. Sutter, M.G. Lagally, *Phys. Rev. Lett.* 82 (1999) 1490.
- [8] W.F. Chung, M.S. Altman, *Ultramicroscopy* 74 (1998) 237.
- [9] M. Mundschaue, E. Bauer, W. Swiech, *J. Appl. Phys.* 65 (1989) 581.
- [10] R.J. Phaneuf, N.C. Bartelt, E.D. Williams, W. Swiech, E. Bauer, *Phys. Rev. Lett.* 67 (1991) 2986.
- [11] E. Bauer, *Rep. Prog. Phys.* 57 (1994) 895.
- [12] M.S. Altman, E. Bauer, *Surf. Sci.* 347 (1996) 265.
- [13] E.Z. Luo, Q. Cai, W.F. Chung, B.G. Orr, M.S. Altman, *Phys. Rev. B* 54 (1996) 14673.
- [14] R.M. Tromp, M.C. Reuter, *Phys. Rev. B* 47 (1993) 7598.
- [15] A.R. Smith, R.M. Feenstra, D.W. Greve, M.S. Shin, M. Skowronski, J. Neugebauer, J. Northrup, *Appl. Phys. Lett.* 72 (1998) 2114.
- [16] A. Pavlovska, E. Bauer, V.M. Torres, J.L. Edwards, R.B.

- Doak, I.S.T. Tsong, V. Ramachandran, R.M. Feenstra, *J. Cryst. Growth* 189/190 (1998) 310.
- [17] A. Pavlovskaya, V.M. Torres, E. Bauer, R.B. Doak, I.S.T. Tsong, *Appl. Phys. Lett.* 75 (1999) 989.
- [18] J.L. Weyher, S. Mueller, I. Grzegory, S. Porowski, *J. Cryst. Growth* 182 (1997) 17.
- [19] R.M. Tromp, M.C. Reuter, *Ultramicroscopy* 36 (1991) 99.
- [20] M.B. Webb, M.G. Lagally, H. Ehrenreich, F. Seitz, D. Turnbull (Eds.), *Solid State Physics: Advances in Research and Applications* Vol. 28, Academic Press, London, 1973, p. 301.
- [21] M. Fink, M.R. Martin, G.A. Somorjai, *Surf. Sci.* 29 (1972) 303.
- [22] G.A. Held, J.D. Brock, *Phys. Rev. B* 51 (1995) 7262.